Surface Species Formed during CO and CO₂ Hydrogenation over Rh/TiO₂ (W⁶⁺) Catalysts Investigated by FTIR and Mass Spectroscopy

Zhaolong Zhang, Angelika Kladi, and Xenophon E. Verykios

*Department of Chemical Engineering, Institute of Chemical Engineering & High Temperature Processes,
University of Patras, GR-26500 Patras, Greece*

Surface species formed over Rh/TiO₂ (W⁶⁺) catalysts during CO and CO₂ hydrogenation were investigated by *in situ* FTIR spectroscopy and transient techniques. It was found that at least four carbon-containing species, namely, linear CO, bridged CO, active carbon (C_α), and less-active carbon (C_β), exist on Rh crystallites, while formate and/or carbonate and/or hydrocarbonate species are on the TiO₂ support. A reduction of CO coverage by 25 ~ 40% and a shift of the linear CO band to higher wavenumber values by 10 ~ 14 cm⁻¹ were observed under CO and CO₂ hydrogenation upon doping the TiO₂ carrier with small amounts of W⁶⁺ cations (<1 at.%). This implies that the Rh–CO bond is significantly weakened by doping, presumably due to an alteration of the electronic structure of the TiO₂ carrier, which modifies the electronic state of surface Rh via electronic interactions at the metal–support interface. The concentrations of the C_α and C_β species on Rh crystallites and carbon-containing species on the support were also found to be influenced by doping. While the concentration of the C_α species (including CH_X species) was reduced and that of the C_β species was enhanced with increasing W⁶⁺ dopant content, the concentration of the carbonate and/or hydrocarbonate species on the carrier exhibited a maximum at a W⁶⁺ content of 0.11 ~ 0.22 at.%. It is reasoned that hydrogen chemisorption is favored on the doped catalysts, as the CO coverage and the strength of the Rh–CO bond are significantly reduced. This has twofold consequences which result in a large increase of the CO and CO₂ hydrogenation activity, as previously observed over the Rh/TiO₂ (W⁶⁺) catalysts: there is an increase in the concentration of surface hydrogen participating in the rate-determining step and an enhancement of the formation of Rh carbonyl hydride species, through which the reaction proceeds via a route of lower activation energy (H-assisted CO dissociation). © 1995 Academic Press, Inc.

INTRODUCTION

Hydrogenation of carbon monoxide and carbon dioxide is of interest from the aspect of use of carbon sources for the synthesis of oxygenates and hydrocarbons. During the last decade, a large number of studies have been conducted on the hydrogenation of carbon oxides over various supported metal catalysts, especially over noble metal catalysts (1–10). It has been demonstrated (5–7) that CO₂ hydrogenation is more active and selective towards methane formation than CO hydrogenation. The activation energy of CO₂ hydrogenation is generally lower than that of CO hydrogenation under analogous conditions. It is now generally accepted (7–9) that CO₂ hydrogenation proceeds via dissociation of the CO₂ molecule to some form of adsorbed CO and then follows the same reaction pathway as CO hydrogenation. However, there still exist many controversies concerning differences in the kinetic behaviors of CO and CO₂ hydrogenation, in spite of the similar pathways of the two reactions (7–10).

Rhodium is an excellent catalyst for hydrogenation reactions, usually exhibiting very high activity, as compared to other metals (7–11). Rhodium supported on various oxides has been applied as catalyst in CO_X ($x = 1$ and 2) hydrogenation. It has been shown that, by manipulating the support of Rh crystallites, activity and selectivity can easily be altered so that desirable products may be obtained (6, 7, 12–14). Solymosi *et al.* (15) investigated the hydrogenation of CO and CO₂ over Rh dispersed on TiO₂ doped with altervalent cations (Mg²⁺, Al³⁺, and W⁶⁺). It was found that a significant alteration of activity and selectivity of CO and CO₂ hydrogenation is obtained by appropriate doping of the TiO₂ carrier. Recent studies conducted in this laboratory (16, 17, 18) showed that the chemisorptive behavior of CO and H₂ over Rh catalysts is also significantly altered by doping of the TiO₂ carrier. The intrinsic activities of CO and CO₂ hydrogenation over Rh are also enhanced by a factor of 20–30 by doping the TiO₂ carrier with a small amount (<1.0 at.%) of W⁶⁺ cations. Moreover, it has been demonstrated that the enhanced catalytic activity over the doped catalysts is not related to the SMSI phenomenon (18). Since the amount of dopant is small

(< 1.0 at.%) and since most of the dopant is incorporated into the matrix of the parent oxide, it is hardly possible that the dopant species directly participate in surface chemistry. Rather, the pronounced influence is most likely due to electronic interactions between the supported metal crystallites and the semiconducting carrier (15–18). It is argued that the greatly enhanced activity caused by carrier doping may be accompanied by significant changes in the concentration and/or type of intermediate species of the reactions studied. Preliminary CO–TPD experiments conducted in this laboratory (16) indicate that the enhanced activities of the hydrogenation reactions are related to weakening of the Rh–CO bond caused by doping of the carrier. Weakening of the Rh–CO bond implies strengthening of the C–O bond, which appears not to conform with the observation that the activity of the hydrogenation reaction, a process requiring dissociation of the C–O bond, is increased by doping of the carrier. Apparently, a contradiction between the experimental results and the prevailing mechanistic explanation exists. Therefore, it is of interest to conduct surface studies by FTIR and mass spectrometry on the Rh/TiO_2 (W^{6+}) catalysts to thoroughly investigate the relationship between enhanced catalytic activity and variation of intermediate species on the surface. This approach is helpful in elucidating the reaction mechanisms of CO_X hydrogenation and the intrinsic nature of the promotional effect of doping of the TiO_2 carrier on catalytic activity.

The infrared spectroscopic technique has been successfully applied in the investigation of surface species formed during hydrogenation of carbon oxides over Rh (19, 20), Pd (21), and Ru (22). Adsorbed CO on the metal crystallites and formate species on the carrier were found to be the major surface carbon-containing species under reaction conditions. Transient MS techniques have also been employed to reveal surface species formed during reaction, particularly for hydrogenation of CO over supported metal catalysts (23–26). Two types of carbon species (other than adsorbed CO and formate) were reported to be present on the working Rh/Al_2O_3 catalyst surface following exposure to CO/H_2; these are an active carbon species, proposed to lead to formation of hydrocarbons, and an inactive carbon species, responsible for blocking of the catalytic sites, resulting in catalyst deactivation. In the present study, the surface species formed during CO and CO_2 hydrogenation over the Rh/TiO_2 (W^{6+}) catalysts are investigated, employing infrared and transient MS techniques. Attention is focused on the influence of carrier doping on the alteration of surface species over the supported Rh catalysts, and on the correlation between the alterations of surface species and the enhancement of catalytic activity which was observed previously (17, 18).

EXPERIMENTAL

A. Catalyst Preparation

Preparation and characterization of the doped TiO_2 supports and Rh catalysts used in the present investigation have been described in detail elsewhere (16, 27). Briefly, to prepare the doped TiO_2 supports, weighed amounts of TiO_2 and WO_3 dopant were slurried with distilled water and thoroughly mixed. The water was evaporated and the residue was dried overnight at 110°C, and then fired in air at 900°C for 5 h. The TiO_2 matrix was converted into the rutile form due to the high temperature treatment, as revealed by XRD measurements (16, 27). Rh catalysts were prepared by incipient wetness impregnation of the support with appropriate amounts of aqueous solutions of $RhCl_3$ at approximately 100°C, and then reduced in flowing hydrogen at 200°C for 2 h.

The Rh content of the catalysts employed in the present study was invariably 0.5 wt.%. The surface area of the support was approximately 10 m^2/g, while the Rh dispersion was found to be ca. 40%, which corresponds to a value of ca. 17.8 μmol Rh surface atoms/g of catalyst. Adding small amounts of W^{6+} dopant (<1 at.%) does not result in any significant alteration in Rh dispersion. The catalysts are designated as 0.5% Rh/TiO_2 (x% W^{6-}), where x is the dopant content of the carrier in at.%.

B. Infrared Spectroscopic Study

A Nicolet 740 FTIR spectrometer equipped with a DRIFT (diffuse reflectance infrared Fourier transform) cell was used for the present in situ measurements. The cell, containing ZnSe windows which were cooled by water circulating through blocks in thermal contact with the windows, allowed collection of spectra over the temperature range 25–300°C, at atmospheric pressure. For all spectra reported, a 32-scan data accumulation was carried out at a resolution of 4.0 cm^{-1}. During the measurements, the external optics were continuously purged with dry nitrogen in order to minimize the level of water vapor and carbon dioxide in the testing compartment. An IR spectrum obtained under He flow at the reaction temperature was used as the background to which the spectrum, after exposure to the reaction feed, was ratioed.

Fifty to approximately seventy milligrams of sample which had been previously finely powdered was placed onto the sample holder. The sample surface was carefully flattened in order to obtain high IR reflectivity. Before exposure to the reaction gas, the sample was pretreated at 300°C under H_2 flow for 1 h and then under He flow for half an hour. The coverage of CO is derived by normalizing the intensity of the CO band to that of the catalyst saturated with CO at 100°C, a compromise temperature at which neither the disruption of Rh–Rh bonds, induced

by CO, nor the Boudouard reaction (CO disproportionation) is significant (28, 29).

C. Transient Kinetic Study

The transient apparatus consists of a switching system which allows one to abruptly switch the feed gas stream, a heated reactor, and an analysis system. The reactor is a quartz tube of 0.6 cm in diameter and 15 cm in length. A section at the center of the tube is expanded to 1.2 cm in diameter, in which the catalyst sample, approximately 250 mg, was placed. Temperature was controlled by a linear temperature programmer (Omega, CN 2010). The outlet of the reactor is connected to a quadrupole mass spectrometer (Sensorlab 200D-VG Quadrupoles) via a heated silica capillary tube of 2 m in length. The pressure in the main chamber of the mass spectrometer is approximately 10^{-7} mbar. The mass spectrometer was connected to a personal computer for instrument control, data acquisition, and analysis. H_2, CH_4, CO, and CO_2 were recorded at m/z = 2, 15, 28, and 44, respectively.

The gases used were of ultrahigh purity. Helium was further purified through a heated metallic zirconium trap, H_2 through an Oxisorb and a molecular sieve 5A trap. The desired gas mixtures were prepared in a separate apparatus, and not by continuous blending of two streams, to avoid changes in gas composition upon switching the valves. Flow rates were controlled at 30 ml/min (ambient). Before introduction of the feed mixture, the sample was preteated at 300°C in H_2 flow for 1 h. 1% Ar was added into the mixture. The Ar transient response, upon switching of the feed gas mixture, was monitored and used in the baseline correction. H_2 was used to titrate the surface carbon-containing species formed after exposure to the feed gases. The titration was carried out in both the isothermal and temperature-programmed modes. The quantities of gaseous products (CH_4, CO, and CO_2) formed under H_2 titration were used to estimate the quantities of surface species. Calibration of the mass spectrometer was performed with a mixture of known composition. The output signal from the mass spectrometer detector was then converted to mole fraction versus time by appropriate software.

RESULTS

In situ infrared spectroscopic results obtained under CO and CO_2 hydrogenation over Rh/TiO₂ (W⁶⁺) catalysts are presented, followed by results of CO_2 hydrogenation obtained by transient mass spectroscopic techniques. A similar transient study concerning CO hydrogenation has been reported recently (17). Also, numerous studies concerning surface carbon-containing species formed during CO hydrogenation over supported Rh catalysts have been published (24, 26, 30). Related results reported in previous
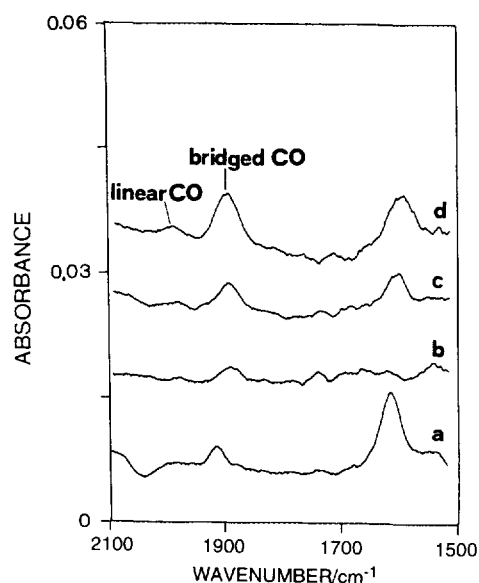

FIG. 1. Infrared spectra of: (a) Rh/TiO₂ (anatase), (b) Rh/TiO₂ (0.0 at.% W⁶⁺), (c) Rh/TiO₂ (0.22 at.% W⁶⁺), (d) Rh/TiO₂ (0.45 at.% W⁶⁺) following exposure to 20% CO₂/He at 235°C.

studies will be referred to and evaluated with respect to the present results, where appropriate.

A. Infrared Spectroscopic Experiments

The surface species formed upon interaction of Rh/TiO₂ ($x\%$ W⁶⁺), x = 0, 0.11, 0.22, 0.45, and 0.67 at.%, with CO_2, CO_2/H_2, and CO/H_2 were investigated by FTIR spectroscopy. For comparison, the Rh/TiO₂ (anatase, without high temperature treatment) catalyst was also employed in the present study under identical conditions. Particular attention was paid to monitoring changes in the coverage and bond strength of adsorbed CO species with respect to doping of the carrier since CO dissociation is proposed to be the rate-determining step for both CO and CO_2 hydrogenation. The bands of surface species formed on the Rh/TiO₂ (W⁶⁺) catalysts were found to develop with time of exposure. Unless indicated otherwise, the spectra shown were obtained after the bands were fully developed and stable, a process which required 10 to 60 min of exposure of the catalyst to the reactant gases.

A1. Interaction of CO_2 with Rh/TiO₂ (W⁶⁺) surfaces. In the absence of H_2, the interaction of CO_2 with Rh/TiO₂ (anatase) at 235°C results in the development of bands at 1620 and 1917 cm⁻¹ (Fig. 1a). Since the position of the band at ca. 1620 cm⁻¹ is close to the band due to adsorbed water (31), this could be adsorbed water, originating from water impurities in the gas phase. The weak band at ca. 1917 cm⁻¹ could be assigned to bridged CO on the Rh crystallites (32, 33). There is a small negative band around 2070 cm⁻¹, which may be caused by small changes in the
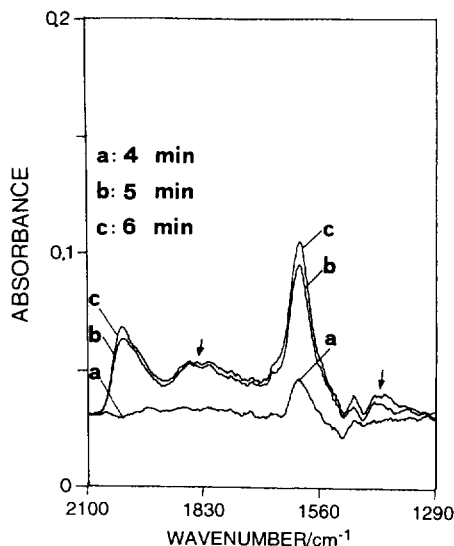
FIG. 2. Development of the CO and formate bands with time on stream upon exposure of the Rh/TiO₂ (anatase) catalyst to CO₂/H₂/He at 235°C: (a) 4 min, (b) 5 min, (c) 6 min.

spectrum background during testing. As a result, distinguishing the linear CO band, if one exists, is difficult.

Similarly, two bands at 1570–1600 and 1900–1920 cm⁻¹ were observed over the surfaces of the Rh/TiO₂ (x at.%, W^{6+}) catalysts, following exposure to CO₂ at 235°C (Fig. 1b, 1c, and 1d). The band at 1570–1600 cm⁻¹ may be due to adsorbed water, or carbonate or hydrocarbonate species (31). A weak dependence of the position and intensity of the bridged CO band on the dopant content seems to exist. However, such alterations should be reserved, because the band is rather broad and weak. In addition to the two bands at 1570–1600 and 1900–1920 cm⁻¹, a weak band which corresponds to linearly bound CO species is also observed at ca. 2043 cm⁻¹ on the Rh/TiO₂ (x at.% W^{6+}) catalysts.

A2. Interaction of CO₂/H₂ with Rh/TiO₂ (W^{6+}) surfaces. The interaction of CO₂/H₂ over the Rh/TiO₂ (anatase) catalyst at 235°C resulted in spectral features at 2043, 1900, 1617–1625, and 1403 cm⁻¹ (Fig. 2). The bands at 1617–1625 and 1403 cm⁻¹ are due to the carbonate and/or hydrocarbonate species on the carrier surface, while the spectral features at 2043 and 1900 cm⁻¹ are due to the formation of the linear and bridged adsorbed CO on the Rh crystallites, respectively. The twin bands of the gem dicarbonyl species, which is the dominant adsorbed CO species at room temperature during CO chemisorption on the Rh catalysts, are not observed. These observations are in agreement with those reported in previous studies involving Rh/TiO₂ and Rh/Al₂O₃ (5, 7, 20, 33). Unlike the case of Rh/Al₂O₃ (7, 20, 33), formate species which should appear at ca. 1586 and 1375 cm⁻¹ do not exist on the present

Rh/TiO₂ catalysts, following the CO₂/H₂ reaction. This is in agreement with the earlier observation made by Henderson and Worley (5) over Rh/TiO₂ catalysts. Although special attention was given to the region 2800–3100 cm⁻¹ where the surface CH$_X$ species are expected to appear, no detectable bands due to CH$_X$ species were observed. This confirms that no (or only very small amounts of) formate species are present on the Rh/TiO₂ catalysts (34, 35).

Similar spectral features were observed over the Rh/TiO₂ (W^{6+}) catalysts, except for differences in band intensity. Figure 3 shows the influence of carrier doping on the spectral features in the region 1700–2100 cm⁻¹. The bands at ca. 2044–2058 and 1880–1920 cm⁻¹ are due to the linear and bridged adsorbed CO species, respectively. The dependence of CO coverage and band position of the linearly adsorbed CO on dopant content is given in Table 1. The band due to the bridged CO is broad and weak, thus any shift caused by carrier doping cannot be safely evaluated. For this reason, the corresponding results are not included in Table 1. It is shown that the intensity of the band due to the linearly adsorbed CO species decreases with increasing dopant content, corresponding to a decrease of CO coverage from 0.3 to 0.16. The wavenumbers of the linearly adsorbed CO species shift to higher values as the dopant content increases. Such a shift is more pronounced at low doping levels.

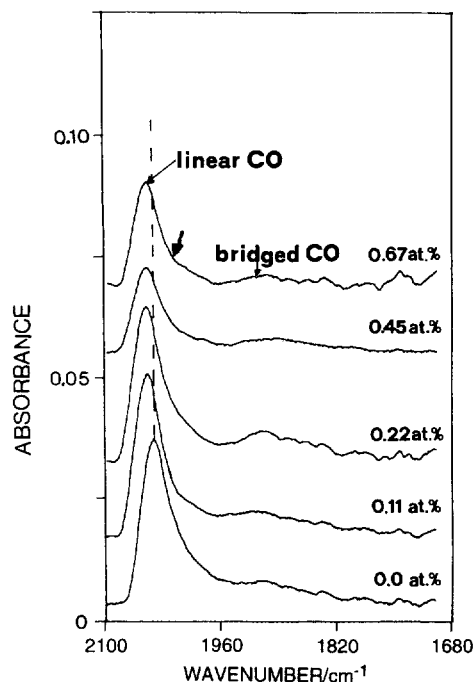It is noted that the band of linearly adsorbed CO devel-

FIG. 3. Infrared spectra of the Rh/TiO₂ (x at.% W^{6+}) catalysts, x = 0.0, 0.11, 0.22, 0.45, and 0.67, following exposure to CO₂/H₂/He at 235°C, for 60 min.

TABLE 1

Wavenumber and Coverage of the Linearly Bound CO Species Formed on Rh/TiO₂ (W⁶⁺) Catalysts during CO₂ and CO Hydrogenation

0.5 wt.% Rh/TiO₂ (W⁶⁺) W⁶⁺ content/at.%	Reaction[a]	Linear CO species	
		Wavenumber (cm⁻¹)	Coverage (θ_{CO})
0	CO₂/H₂	2044	0.30
0.11		2054	0.28
0.22		2054	0.27
0.45		2056	0.15
0.67		2058	0.16
0	CO/H₂	2053	0.60
0.67		2063	0.45

[a] Reaction was carried out at 235°C.

oped upon CO₂/H₂ reaction at 235°C (Fig. 3) is significantly asymmetric, and is characterized by a shoulder on the side of lower wavenumbers, as compared to spectra obtained upon chemisorbing CO alone (28). This suggests that the surface contains more than one type of linearly adsorbed CO species, with variable C–O bond strength. The component of the linearly adsorbed CO giving rise to the shoulder-band at lower wavenumbers may be a CO species which is associated with adsorbed hydrogen species. It is well-known (19, 29, 33) that the Rh carbonyl hydride species has a lower wavenumber than the respective adsorbed Rh carbonyl species. This is due to charge transfer from the bonded hydrogen(s) to the Rh center, enhancing the π donation from Rh into an antibonding π orbital of CO. Consequently, the C–O bond is weakened. Earlier studies conducted in this laboratory (28, 29) show that a shift of the CO band to lower frequencies occurs when the CO-covered Rh/TiO₂ catalyst is exposed to H₂. When CO chemisorbs on the H-covered Rh/TiO₂ catalyst, the CO band is also found to be at lower frequencies. However, as the preadsorbed H-species is gradually replaced by CO, the CO band is shifted to higher frequencies, approaching the position of the CO band originating from CO chemisorption on clean Rh/TiO₂. These results confirm that the association of hydrogen species makes the CO band shift toward lower frequencies. Since the shoulder CO band at lower frequencies is only observed when H₂ is cochemisorbed, it is reasonably proposed that it corresponds to the CO species associated with adsorbed hydrogen species. Unfortunately, this band is heavily masked by the intense linear CO band, making a comparison of the relative population of the Rh carbonyl hydride species over the various catalysts difficult, if not impossible. Earlier transient isotopic studies (24, 26) also showed that the amount of carbonyl

hydride species on the supported Rh catalyst, formed during CO_X hydrogenation, is negligibly small, as compared to the coverage of CO species. The present results seem to be in agreement with previous observations [24, 26].

By monitoring the variation in wavenumber and intensity of the CO band with time on stream (within the initial 1–2 h of the CO₂/H₂ reaction), it was found that the band intensity was increased and the wavenumbers of adsorbed CO gradually shifted to higher values with increasing time on stream. The frequency shift is as high as 24 cm⁻¹ in the case of the Rh/TiO₂ (0.11 at.% W⁶⁺). Figure 4 shows the variation of the spectra of adsorbed CO over the Rh/TiO₂ (0.11 at.%. W⁶⁺) catalyst with time on stream. The gradual shift in frequency of the C–O bond may be related to alterations in the dipole–dipole interactions of two neighboring adsorbed CO species, as well as in the surface electronic state during reaction (36, 37). It is interesting to note that the time it takes to reach a stable wavenumber of the adsorbed CO is strongly affected by carrier doping. While more than 1 h time on stream is required for the undoped catalyst to reach a stable wavenumber of the adsorbed CO band, the corresponding time is shortened to less than 40 min for the doped catalysts. This observation suggests that the capability of the catalyst to reach a steady state during reaction is significantly affected by carrier doping.

A3. Interaction of CO/H₂ with Rh/TiO₂ (W⁶⁺) surfaces. The spectra obtained during CO/H₂ reaction at 235°C over the doped and undoped Rh/TiO₂ catalysts are shown in Fig. 5. The bands at 2180 and 2122 cm⁻¹ are due
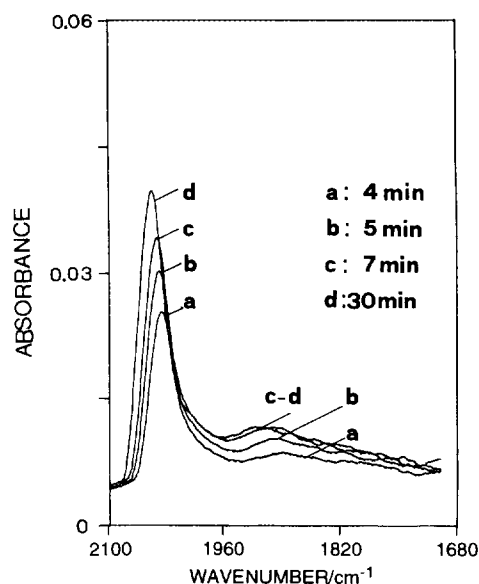

FIG. 4. Development of the CO bands with time on stream upon exposure of the Rh/TiO₂ (0.11 at.% W⁶⁺) catalyst to CO₂/H₂/He at 235°C: (a) 4 min, (b) 5 min, (c) 7 min, (d) 30 min.
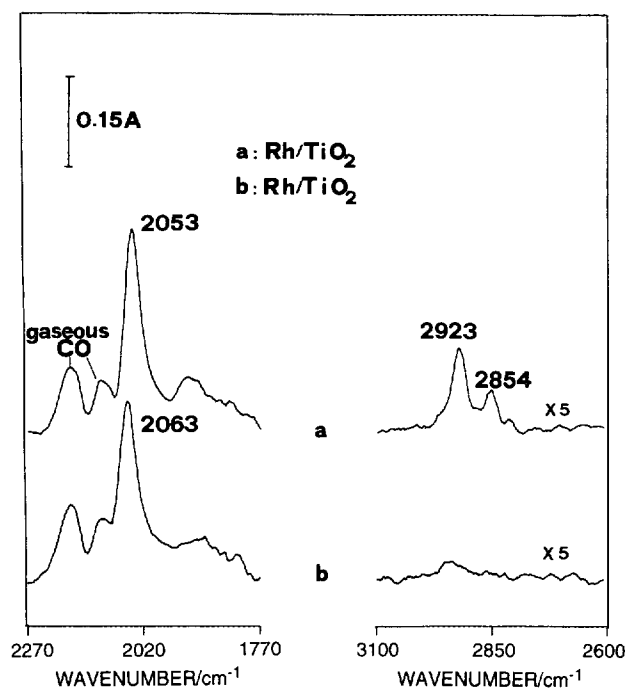
FIG. 5. Infrared spectra of (a) Rh/TiO₂ (0.0 at.% W⁶⁺) and (b) Rh/TiO₂ (0.67 at.% W⁶⁺) following exposure to CO/H₂ at 235°C, for 60 min.

to the P and R branches of the gaseous CO vibration, respectively. The main adsorbed CO band is around 2050–2060 cm⁻¹, which corresponds to the linearly adsorbed CO on Rh crystallites. It was observed that, as a result of carrier doping ($x = 0.67$ at.%), the wavenumber of this band is increased from ca. 2053 to 2063 cm⁻¹, whereas the corresponding CO coverage, θ_{CO}, is reduced from ca. 0.60 to 0.45 (Table 1). A broad band at ca. 1890 cm⁻¹ also exists which should be assigned to the bridged CO species. The twin bands due to the gem dicarbonyl species are not observed on the working catalyst surface, as in the case of CO₂ hydrogenation. A weak band at 1545–1585 cm⁻¹ was also observed (not shown) over the doped and undoped Rh/TiO₂ catalysts, presumably due to formate species on the carrier which result from interaction of CO with surface hydroxyl groups. The low concentration of formate species should be attributed to the low surface area of the Rh/TiO₂ (W⁶⁺) catalysts which have been treated at high temperatures. Since the band due to the symmetric O–C–O stretching of formate species (at ca. 1370 cm⁻¹) is usually much weaker than the asymmetric one (at ca. 1580 cm⁻¹), failure to detect the symmetric band in the present study is reasonable. It is noted that, similar to the case of CO₂/H₂ reaction (Fig. 3), the linear CO band obtained is also asymmetric, although to a smaller extent. Similarly, it can be proposed that the shoulder band at the lower wavenumbers may correspond to the Rh carbonyl hydride species.

In contrast to the case of CO₂ hydrogenation, two bands

due to C–H bonds were detected under CO hydrogenation. As shown in Fig. 5, along with changes in the adsorbed CO species, an alteration in the bands of the C–H bond with carrier doping is also registered. While two bands at 2854 and 2923 cm⁻¹ with substantial intensity are observed on the undoped catalyst, only a very weak band at ca. 2924 cm⁻¹ is observed on the doped catalyst (Fig. 5). As mentioned above, the concentration of formate species is low. Its corresponding C–H band should be weak, even possibly too weak to be detected. Previous experiments (7, 12) on chemisorption of formic acid on Rh catalysts show that only one C–H band at ca. 2900–2920 cm⁻¹, corresponding to formate species on the support, is observed. It was reported by Rethwisch and Dumesic (31) that the presence of formate species on TiO₂ only gives one C–H band at ca. 2920 cm⁻¹. In the present study, two bands at 2923 and 2854 cm⁻¹ are detected on the undoped Rh catalyst. Apparently, they cannot be attributed to the C–H bond of the formate species. Since a previous kinetic study failed to detect any methanol formation from the CO/H₂ over the Rh/TiO₂ (W⁶⁺) catalysts (17), the two C–H bands cannot be attributed to surface methoxy species either. On the other hand, the position and separation (70 cm⁻¹) of these two bands (Fig. 5) neatly fits the -CH_X- species, leading to the suggestion that hydrocarbon fragments exist on the Rh catalysts during CO hydrogenation. The surface (-CH_X-) species are the building blocks for development of carbon chains. It can be derived, therefore, that the concentration of the hydrocarbon fragments on the undoped catalyst is higher than that on the doped catalyst. This offers a good explanation of an earlier finding (17) that selectivity to higher hydrocarbons is reduced by doping the TiO₂ carrier with W⁶⁺ cations.

B. Transient Kinetic Experiments

B1. Interaction of CO₂ with the catalyst surface. The interaction of CO₂ with the Rh/TiO₂ (W⁶⁺) catalysts in the absence of H₂ was investigated within the temperature range 200–300°C. No detectable CO was found to evolve into the gas phase when CO₂ was passed over the catalyst. This is in agreement with the present IR results (Fig. 1), which show a very weak linearly adsorbed CO band, following exposure of the catalyst to CO₂ (there exists a weak CO band at ca. 1920 cm⁻¹, which corresponds to strongly bonded bridged CO species). However, a small amount of CO₂ and CO desorbing from the Rh catalyst was registered when the feed gas was switched from CO₂ to He at $T \geq$ 250°C, indicating that the adsorbed CO and the carbon-containing species (carbonate and/or hydrocarbonate) on the carrier could desorb and/or partially decompose under He flow at the temperatures used. The extent of CO_X desorption was found to be affected, to a certain extent, by temperature as well as dopant content. Therefore, the
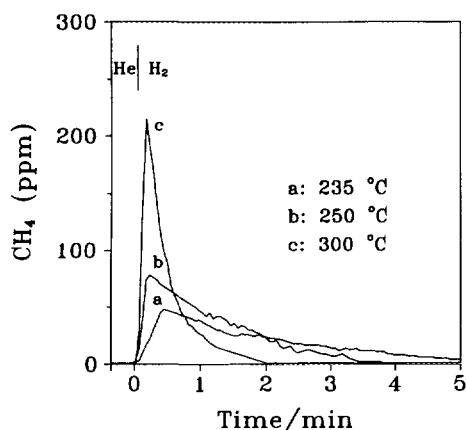
FIG. 6. Transient response of CH₄ over Rh/TiO₂ (0.67 at.% W⁶⁺) catalyst at 235–300°C, according to the delivery sequence CO₂ (100 s) → He (60 s) → H₂ (t).

quantity of surface carbon species (the surface carbon-containing species which can be evolved as methane by H₂ titration under the conditions stated) estimated by H₂ titration (following the delivery sequence He → CO₂ → He → H₂ titration), may be somewhat underestimated, compared with the actual quantities of carbon species formed under CO₂ atmosphere. However, the desorption of the adsorbed species was not found to be significant, as long as the temperature of the He purge was low enough (≤235°C) and the purge time was short (1 min), which is in agreement with a previous observation (24).

Figure 6 shows transient responses of CH₄, following H₂ titration (isothermal) of the Rh/TiO₂ (0.67 at.% W⁶⁺) catalyst which was exposed to CO₂ at various temperatures for a fixed period of time, 100 s. It can be seen that the quantity of surface carbon species increases with increasing reaction temperature, as indicated by an increasing amount of CH₄ evolving from the surface. At the highest temperature studied (300°C, Fig. 6c), there is an initial sharp increase in the rate of production of methane as H₂ starts to flow over the CO₂-exposed surface. This is followed by a quick decrease in the rate of production of methane which lasts for about 2 min. Decreasing temperature results in reduction of the initial rate of CH₄ production and a shift in the appearance of the maximum of the CH₄ peak towards longer reaction times in H₂ flow (Fig. 6, curves a and b). Similar peak shapes were obtained over the un-doped catalysts and the catalysts with other doping levels (not shown). The alteration of the intensity of the methane response at various temperatures with carrier doping is summarized in Table 2. It is found that the intensity of the methane transient response and its sensitivity to temperature are significantly affected by dopant content. Note that the concentration of the carbonate and/or hydrocarbonate

TABLE 2

Quantity of Surface Carbon-Containing Species Derived from Isothermal H₂ Titration of CO₂-exposed Rh/TiO₂ (W⁶⁺) Catalysts at Various Temperatures.[a]

Catalyst Rh/TiO₂ (x at.%, W⁶⁺)	Quantity of CH₄/μmol·g$_{cat}^{-1}$		
	235°C	250°C	300°C
0	0.73	1.32	2.50
0.11	0.82	1.78	3.72
0.22	0.94	2.03	3.91
0.45	1.21	2.10	3.72
0.67	0.95	1.98	3.40

[a] The exposure time to CO₂ was 100 s.

species is affected by the dopant content, as shown in the present IR study (Fig. 1).

B2. Interaction of CO₂/H₂ with the catalyst surface. Figure 7 shows CH₄ transient responses, following H₂ titration (isothermal) of the Rh/TiO₂ (0.22 at.% W⁶⁺) catalyst which was exposed to CO₂/H₂ and CO₂ at 235°C. The quantity of CH₄ evolving from the CO₂/H₂-exposed catalyst is about 24.4 μmol/g$_{cat}$, which is roughly 26 times higher than that from the CO₂-exposed catalyst. This is in agreement with the IR results which show enhancement of the bands due to the linear CO and the carbonate and/or hydrocarbonate species on the CO₂/H₂-exposed catalyst. Apparently, the formation of carbonate and/or hydrocarbonate and adsorbed CO species from CO₂ is promoted by H₂. It is noted that two peaks (designated 1 and 2 in Fig. 7, curve b) are evolved from the CO₂/H₂-exposed catalyst, while only a single peak is produced
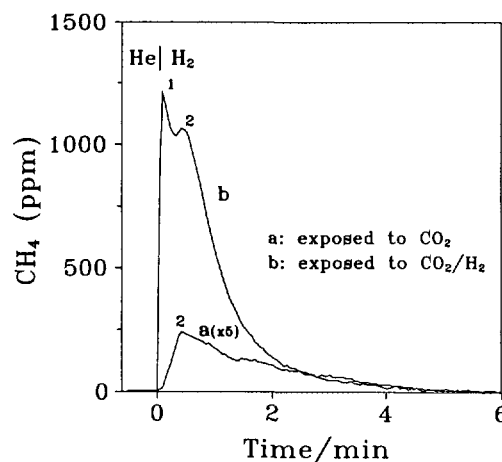

FIG. 7. Transient response of CH₄ over Rh/TiO₂ (0.22 at.% W⁶⁺) catalyst at 235°C, according to the delivery sequences: (a) CO₂ (100 s) → He (60 s) → H₂ (t), (b) CO₂/H₂ (100 s) → He (60 s) → H₂ (t).
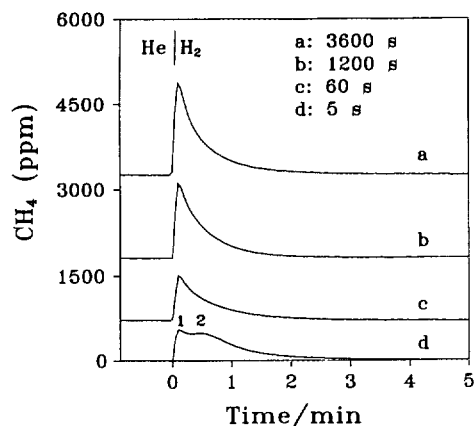
FIG. 8. Transient response of CH$_4$ over Rh/TiO$_2$ (0.67 at.% W^{6+}) catalyst at 235°C and various exposure times, according to the delivery sequence CO$_2$/H$_2$ (5–3600 s) → He (60 s) → H$_2$ (t).

from the CO$_2$-exposed catalyst (Fig. 7, curve a). In the former case, the rate of methane production is very large, as compared to the latter case. Also, based on the time required to reach the peak maximum, the peak in Fig. 7a is associated with peak 2 in Fig. 7b. This suggests that there exists a new carbon-containing species (peak 1) on the CO$_2$/H$_2$-exposed catalyst, which is more active than the carbon-containing species on the CO$_2$-exposed catalyst. Figure 8 shows the influence of time of exposure to the CO$_2$/H$_2$ mixture on the transient response of methane from the Rh/TiO$_2$ (0.67 at.% W^{6+}) catalyst surface. It is shown that the two peaks, peak 1 and peak 2, are partially resolved at low exposure time only. As the intensities of the two peaks increase with increasing time of exposure, peaks 1 and 2 heavily overlap. The quantity of methane evolved from the surface tends to be stable after 20–60 min of reaction, which is in good agreement with the present IR study which shows that the bands of surface species become stable following 30 min of exposure to the CO$_2$/H$_2$ mixture (Fig. 4).

In order to separate peaks 1 and 2, the following deconvolution procedure was used (24, 30). Following exposure to CO$_2$/H$_2$ at a specific reaction temperature (235°C in most cases) for 1200 s, the system was quickly quenched in helium to 100°C. Then the feed was switched to H$_2$ for the isothermal titration (at 100°C) for 120 s. After this, the temperature of the system was increased at a rate of 17°C/min, and the TPR was carried out. This methodology allows one to distinguish different surface carbon species of variable reactivity since they start to be reactive towards H$_2$ at different temperatures. Figure 9 shows the transient response of CH$_4$ from the Rh/TiO$_2$ (0.11 at % W^{6+}) catalyst, following the procedure described above. Peak 1 is now resolved from peak 2, appearing as a sharp spike during the H$_2$ isothermal titration at 100°C. Peak 2 evolves at

180–300°C during the subsequent temperature-programmed exposure to H$_2$. The formate and carbonate and/ or hydrocarbonate species have been reported to be reactive toward H$_2$ in the range 170–350°C (26, 38). In a previous study of CO-TPR over Rh/TiO$_2$ catalysts (39), methane evolution (hydrogenation of the adsorbed CO) was found to occur at 150–200°C. The temperature at which formate, carbonate and/or hydrocarbonate, and absorbed CO are reactive towards H$_2$ falls within the temperature range in which the broad peak, peak 2, is evolved. It can thus be derived that the active carbon-containing species, peak 1, corresponds to neither adsorbed CO nor adsorbed carbonate and/or hydrocarbonate. This species (peak 1) is defined as an active carbon C$_\alpha$ which most probably originates from the dissociation of adsorbed CO. The broad peak is considered to consist of contributions from adsorbed CO and carbonate and/or hydrocarbonate species. In the present study, these peaks cannot be easily resolved. Actually, the quantity of CH$_4$ under the broad peak (peak 2) is equivalent to more than one (1.2–1.6) monolayers of carbon species on the Rh crystallites (assuming C/RH$_S$ = 1), which is much higher than that of the adsorbed CO (θ_{CO} = 0.16–0.3) derived by the IR study (Table 1). This suggests that the broad peak is mainly due to carbon-containing species on the carrier, while the contribution of the adsorbed CO amounts to less than ca. 20%.

In order to investigate the existence of inactive carbon species, which might be reactive towards H$_2$ at elevated temperatures, the CO$_2$/H$_2$-exposed surface was further titrated with H$_2$ at higher temperatures, following removal of
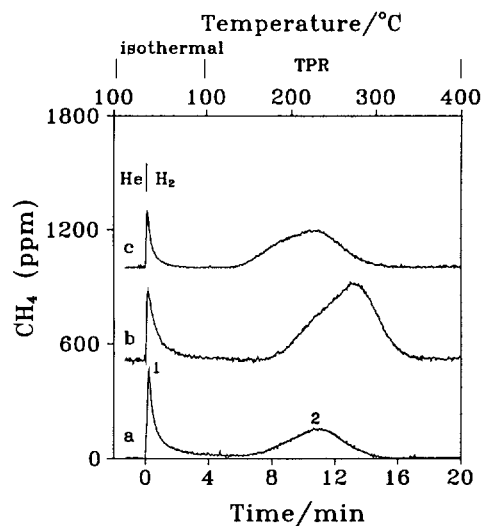
FIG. 9. TPR response of CH$_4$ according to the delivery sequence CO$_2$/H$_2$ (1200 s), T = 235°C → He, cool-down to 100°C → H$_2$ (120 s), T = 100°C → TPR, T = 100–400°C, at a heating rate of 17°C/min: (a) Rh/TiO$_2$ catalyst, (b) Rh/TiO$_2$ (0.22 at.% W^{6+}) catalyst, and (c) Rh/TiO$_2$ (0.67 at.% W^{6+}) catalyst.
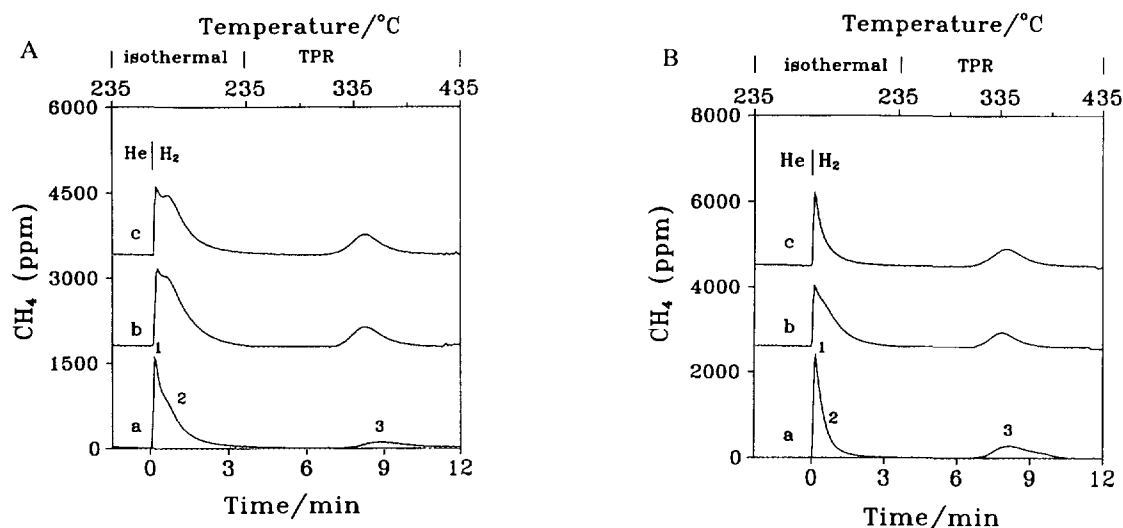
FIG. 10. Transient response of CH₄ at 235°C according to the delivery sequences: (A) CO₂/H₂ (5 s) → He (60 s) → H₂ (t) and (B) CO₂/H₂ (1200 s) → He (60 s) → H₂(t). After the isothermal H₂ reduction at 235°C, TPR is carried out at a heating rate of 25°C/min: (a) Rh/TiO₂ catalyst, (b) Rh/TiO₂ (0.22 at.% W⁶⁺) catalyst, and (c) Rh/TiO₂ (0.67 at.% W⁶⁺) catalyst.

surface carbonate and/or hydrocarbonate, CO, and active carbon (C_α), by the isothermal H₂ titration at 235°C. (It is possible that a portion of carbonate and/or hydrocarbonate does not fully react to CH₄ at the temperature applied.) Figure 10 shows the transient response of methane obtained by the isothermal H₂ titration of the CO₂/H₂-exposed surface (exposure time (Δt) of 5 or 1200 s) at 235°C, followed by TPR at a heating rate of 25°C/min. It is noted that, in addition to peaks 1 and 2, an additional CH₄ peak (peak 3) evolves at higher temperatures (320–360°C from the CO₂/H₂-exposed catalyst. The area under peak 3 is affected by the dopant content and is slightly increased with time on stream (from 5 to 1200 s). The species from which peak 3 originates is unlikely to participate in the reaction schemes for the formation of methane at the low reaction temperatures employed (200–250°C). This species is unlikely to be attributable to adsorbed CO and carbonate and/or hydrocarbonate species on the surface because the latter start to be reactive to H₂ at temperatures below 250°C, as shown above. In previous studies of CO hydrogenation (15, 24), it has been demonstrated that some transformation of active carbon to a less active form occurs over supported Rh catalysts. The less active carbon starts to be reactive towards H₂ at temperatures above ca. 320°C. Therefore, the species corresponding to peak 3 is tentatively assigned to the inactive carbon species, C_β, which probably results from the aging of the active carbon C_α species (i.e., $C_\alpha \rightarrow C_\beta$). As mentioned above, the inactive carbon species also possibly originates from the surface carbonate and/or hydrocarbonate which have survived from the isothermal H₂ titration at 235°C. However, such a possibility is considered to be small since peak 3 does

not appear in the analogous experiments of the CO₂-exposed catalysts.

Similar peak shapes (peaks 1, 2, and 3) with different intensities were obtained over the other Rh/TiO₂ (W⁶⁺) catalysts which had been exposed to CO₂/H₂. Therefore, the transient responses of these samples are not repeatedly shown. Instead, the influence of carrier doping on the quantities of methane under peaks 1, 2, and 3 is summarized in Table 3. It can be seen that the quantity of C_α (peak 1) is slightly reduced whereas the quantity of C_β (peak 3) is appreciably increased with increasing concentration of W⁶⁺ cation in the carrier. The quantity of peak 2, which consists of the adsorbed CO and carbonate and/or hydrocarbonate, initially increases and then decreases with increasing dopant content, exhibiting a maximum at the dopant content

TABLE 3

Coverage of Various Surface Carbon-Containing Species (Peaks 1, 2 and 3) Derived by H₂ Titration of CO₂/H₂-Exposed Rh/TiO₂ (W⁶⁺) Catalyst at 235°C[a]

Catalyst Rh/TiO₂ (x at.%, W⁶⁺)	CH₄ (monolayers)[b]			
	Peak 1	Peak 2	Peak 3	Total
0	0.073	1.05	0.072	1.20
0.11	0.060	1.22	0.090	1.37
0.22	0.053	1.43	0.121	1.60
0.45	0.055	1.35	0.124	1.53
0.67	0.043	1.28	0.131	1.45

[a] The exposure time to CO₂/H₂ mixture was 1200 s.
[b] The value was obtained assuming C/Rhₛ = 1.

of 0.11–0.22 at.%. As shown by the IR study, the quantity of adsorbed CO decreases with increasing dopant content (see Fig. 3 and Table 1), which does not conform to the above pattern. This may be due to the small fraction of the adsorbed CO in peak 2 (less than ca. 20%), which does not significantly affect the pattern of the total dependence (formate plus CO species). It is then implied that the quantity of the carbonate and/or hydrocarbonate species on the carrier is affected by carrier doping, having a maximum at dopant contents of 0.11–0.22 at.%.

DISCUSSION

A. Influence of Carrier Doping on Surface Carbon-Containing Species

The influence of carrier doping on the surface carbon-containing species, formed during CO_2 and CO hydrogenation, has been presently investigated employing infrared and transient MS techniques. While the IR study discloses the formation of adsorbed CO on the Rh crystallites and carbonate and/or hydrocarbonate on the carrier, the transient kinetic study reveals information concerning the carbon-containing species on the TiO_2 support, as well as various carbonaceous species, e.g., C_α and C_β species on Rh crystallites, originating from C–O dissociation. Through careful evaluation of the results obtained by the two techniques under analogous conditions, a complete picture of the carbon-containing species formed on the catalyst surface during CO_X ($x = 1$ and 2) hydrogenation may be obtained.

A1. CO_2 hydrogenation. As revealed by transient MS studies (Tables 2 and 3), the quantity of carbonate and/or hydrocarbonate formed on the catalyst by interaction with CO_2/H_2 initially increases and then decreases with increasing W^{6+} dopant content, exhibiting a maximum at a dopant content of 0.11–0.22 at.%. This implies that more sites for CO_2 adsorption exist on the carrier containing 0.11 ~ 0.22 at.% W^{6+}. Although the intrinsic reason for such a dependence is presently unclear, it appears that the results are related to the incorporation of W^{6+} cations into the matrix of TiO_2 (the effective ionic radii of W^{6+} and Ti^{4+} are 62 and 68 pm, respectively (40)), which produces defect sites on the carrier surface. These sites tend to easily adsorb CO_2, in the form of carbonate and/or hydrocarbonate species, with participation of hydrogen-containing species.

The quantity of adsorbed CO species on Rh crystallites is found by the IR study to decrease with increasing dopant content (Fig. 3 and Table 1). Also, a shift of the C–O vibrational frequency, to higher wavenumber, by ca. 14 cm^{-1}, is observed. It has been shown by many researchers (29, 36) that a band shift to higher frequency occurs with increasing CO surface coverage due to the enhanced dipole–dipole interaction between neighboring CO mole-

cules. The present IR study shows that the main CO species adsorbed on Rh crystallites is the linearly adsorbed CO, while no gem dicarbonyl species is formed on the surface during CO_2 hydrogenation. Since the shift to higher frequency ("blue shift") is observed for the doped catalysts over which low CO coverages are observed, it is unlikely to be due to enhancement of dipole–dipole interactions. Instead, the blue shift should be attributed to changes in the electronic configuration of the Rh surface, which results in the weakening of the Rh–CO bond or the strengthening of the C–O bond. The alteration of the electronic state of the Rh surface upon carrier doping can be reasonably attributed to the modification of electronic interactions between small Rh crystallites and the carrier. Doping of the TiO_2 carrier with cations of valence higher than that of Ti^{4+} is known to result in a decrease in the work function of the parent oxide (27, 41). According to the theory of metal–semiconductor contacts this intensifies the charge transfer from the doped carrier to the supported Rh crystallites, which have a higher work function than the doped TiO_2 carrier (28, 42, 43). In fact, the reduced CO coverage on the doped catalysts coincides with the weakening of the Rh–CO bond, which favors a partial desorption of CO from the surface. These results are also in good agreement with an earlier CO-TPD study (17) which showed desorption of CO from the doped Rh catalysts at lower temperatures, as compared to that from undoped ones.

As revealed by the present transient study, two types of surface carbon species, C_α and C_β, exist on the Rh surface, after exposure to a CO_2/H_2 feed. Both species most probably originate from dissociation of the C–O bond. While the reaction between the active carbon species, C_α, and hydrogen leads to methane formation, the methanation process is unlikely to involve the participation of the inactive carbon species, C_β, which only becomes reactive towards H_2 at temperatures above 320°C, and may only result in the blocking of a fraction of the surface Rh sites. Since the C_β species is not consumed by hydrogen at the reaction temperature (200–250°C), its quantity is, to a certain degree, related to the extent of aging of the C_α to the C_β species. The fact that the quantity of the C_β species on the Rh surface is increased with increasing dopant content (Table 3) suggests that enhanced aging of C_α to C_β occurs on the doped catalyst. The quantity of the C_α species is mainly determined by the rate constants of the CO dissociation and the reaction of C_α with hydrogen (under steady state, the rate constant of aging of C_α to C_β should be negligibly slow, as compared to that of the other two processes), as well as by the concentration of the surface species concerned. The reduced quantity of C_α species on the doped catalyst implies that either the reaction rate between the C_α species and hydrogen is enhanced or that the dissociation of CO on the doped catalyst is retarded. This subject will be discussed further in the following section.

A2. CO hydrogenation. As revealed by the present IR study (Fig. 5), the concentration of adsorbed CO and hydrocarbon fragments, CH_x, formed during CO hydrogenation on the Rh crystallites, is substantially reduced by doping the TiO₂ carrier with W^{6+} cations. This is in good agreement with the TPO results obtained in a previous study (17), which showed that smaller amounts of CO₂ are evolved from the CO/H₂-exposed doped catalyst than from the corresponding undoped catalyst. It is noted that the wavenumber of the CO band in the case of CO hydrogenation is higher by ca. 10 cm^{-1} than it is in the case of CO₂ hydrogenation (Table 1). This many be attributed to enhanced dipole–dipole interactions due to the high CO coverage of the CO/H₂-exposed surface, as compared to that of the CO₂/H₂-exposed surface. However, the reduction of CO coverage and the blue shift of the wavenumber of the adsorbed CO band, upon doping of the carrier (Fig. 5), should be attributed to alterations in the electronic state of the Rh crystallites, as reasoned earlier. The reduction of the concentration of the hydrocarbon fragments (CH_x) on the surface upon carrier doping seems to be related to enhanced hydrogen coverage, which promotes removal of the hydrocarbon fragments (10, 44). An earlier kinetic study (17) over Rh/TiO₂ catalysts showed that, in addition to methane, higher hydrocarbons (C_{2-6}) were also produced under CO hydrogenation. However, the selectivity towards higher hydrocarbons was significantly reduced by doping TiO₂ with W^{6+} cations. Apparently, this is related to the decreased concentration of hydrocarbon fragments on the surface, which may be due to enhanced hydrogen coverage. Enhanced hydrogen coverage is expected when the strength of CO chemisorption and CO coverage are significantly reduced. This deduction is supported by earlier TPD and FTIR studies (16, 28) of CO adsorption on H-covered surfaces of Rh/TiO₂ (W^{6+}) catalysts, which demonstrated that the displacement of hydrogen species by adsorbing CO molecules is significantly retarded on the doped catalysts, as compared to the undoped ones.

B. Connections between the Alterations of Surface Species and the Kinetic Parameters of CO and CO₂ Hydrogenation

The most pronounced influence of carrier doping on kinetic parameters of CO_x ($x = 1$ and 2) hydrogenation is in the enhancement of the activity of methanation by ca. 20 and 24 times, and in the reduction of the apparent activation energy by ca. 20 and 30 kJ/mol for CO and CO₂ hydrogenation, respectively (17, 18). Such kinetic alterations should be primarily reflected in changes in the concentration and the reactivity of adsorbed CO and C_α species, since the dissociation of CO to C_α is the rate-determining step of the reaction. Although the concentration of carbon-containing species on the carrier is also
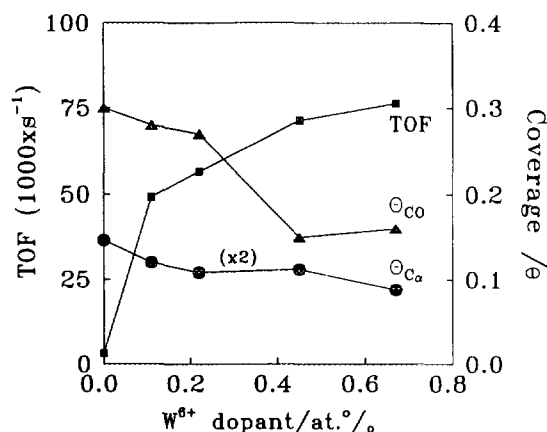

FIG. 11. Dependence of activity of CO₂ methanation and concentration of adsorbed CO and C_α species on W^{6+} dopant content. The concentrations of adsorbed CO and C_α species were derived from the IR study and the transient kinetic study, respectively. The activity of CO₂ methanation was obtained under the reaction conditions $T = 235°C$, CO₂/H₂ = 1/4 (18).

affected by doping, as described above, it is unlikely to result in any significant influence on the formation of hydrocarbons, since the rate of conversion of CO₂ to CO is expected to be much faster than the rate of hydrogenation. However, the selectivity to CO (a side-product of CO₂ hydrogenation) may be affected by the variation of the concentration of the carbonate and/or hydrocarbonate species. In order to better correlate the changes in activity of hydrogenation and in the concentration of surface species, the dependence of the activity of CO₂ methanation and the concentration of the adsorbed CO and C_α species on dopant content is plotted in Fig. 11. It is shown that while activity increases significantly with increasing dopant content, the concentration of adsorbed CO and C_α species decreases with increasing dopant concentration. No correlation between these parameters is apparent unless the following hypothesis is proposed.

According to the mechanism of CO_x hydrogenation proposed previously (5, 18, 20, 33), as well as the surface species identified in the present study, the reaction scheme for CO_x hydrogenation over Rh/TiO₂ (W^{6+}) catalysts may be depicted as follows:
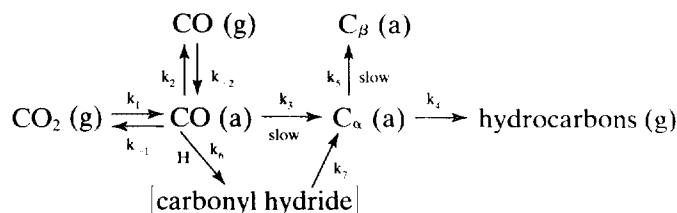
Compared to the C–O dissociation step, conversion of CO_2 to CO (or CO chemisorption on the surface in the case of CO hydrogenation) is a fast step which should not limit the rate of hydrogenation (5, 18, 20). Consequently, a relatively high CO pool on the surface is expected. As shown in the present study, the CO coverage of Rh/TiO_2 (W^{6+}) catalysts ranges from 0.16 to 0.60 for CO_X hydrogenation, which is much large than the corresponding C_α coverage (Table 3). From the kinetic point of view, one may speculate that only a small fraction of adsorbed CO species instantaneously participates in the reaction scheme, while the majority are only "spectator" species or "surface poison" in view of the competitive adsorption of hydrogen. In the case of CO hydrogenation, adsorbed CO species are in equilibrium with gaseous CO, while in the case of CO_2 hydrogenation, adsorbed CO species are in equilibrium with gaseous or adsorbed CO_2. Apparently, relatively high CO coverage is expected in the former case, which is also in agreement with the present observation (Table 1). The C_α species represents the active carbon species which is distinguished from the less active carbon species, C_β, and which may consist of one or more types of carbon species, e.g., CH_X hydrocarbon fragments. The composition and reactivity of the C_α species with H_2 are closely related to the activity and selectivity of the hydrogenation reaction. The present transient study of CO_2 hydrogenation shows that the reactivity of the C_α species with H_2 is very high, as compared to the reactivity of adsorbed CO and carbonate and/or hydrocarbonate species. Therefore, the reaction between the C_α species and surface hydrogen to form hydrocarbons (step 4) is expected to be faster than the dissociation of the C–O bond (step 3). The rate of hydrogenation is thus anticipated to be determined by the slow step of CO dissociation. The strength of the C–O bond over Rh crystallites is enhanced by carrier doping, as indicated by the blue shift of the adsorbed CO band. According to the prevailing view (9, 10), it would be expected that this would increase the activation energy of dissociation of the C–O bond, resulting in reduction of the reaction rate. However, such a deduction is not in agreement with the kinetic results obtained in earlier studies (17, 18), which showed that the apparent activation energy of the reaction is reduced while the reaction rate is increased by carrier doping. Apparently, an alternative explanation should be sought.

It has been demonstrated that the rate of CO dissociation in the presence of hydrogen is much higher than it is in the absence of hydrogen. This is attributed to hydrogen-assisted reduction of the energy barrier for CO dissociation. Since the hydrogen coverage of the doped catalyst is larger than that of the undoped catalyst, it appears that in the former case the dissociation of CO follows, at least partially, a reaction route which involves an Rh carbonyl hydride intermediate. This route (i.e., steps 6 and 7) re-

quires lower activation energy. The above hypothesis is supported by the observation of the shoulder band at the lower wavenumbers of the linear CO band, which presumably corresponds to the Rh carbonyl hydride species on the working surface (Figs. 3 and 5). Previous studies over Rh/TiO_2 catalyst conducted in this laboratory (28, 29) confirm that a shift of the CO band to lower frequencies occurs when the adsorbed CO species is associated with hydrogen species. Based on this hypothesis, the rate of hydrogenation can be expressed by

$$R_{CH_4} = k_6 \cdot \theta_{CO}^n \cdot \theta_H^m. \qquad [1]$$

Since the CO coverage, θ_{CO}, is rather high, as a first approximation, it may be treated as a constant. Therefore, the rate can be further simplified to

$$R_{CH_4} = k_6' \cdot \theta_H^m. \qquad [2]$$

Equation [2] implies that a key way to enhance activity is to increase the hydrogen coverage on the working catalyst surface. This is in harmony with a previous kinetic study (18) on Rh/TiO_2 (W^{6+}) catalyst, which showed that the rate of CO_2 hydrogenation is nearly linearly dependent on hydrogen partial pressure, at low H_2 partial pressures. Due to the high affinity of CO for metal surfaces, CO adsorption prevails under conditions of competitive adsorption with hydrogen. Therefore, the CO coverage is expected to be much higher than that of hydrogen. Earlier transient studies by Efstathiou and Bennett (24) have shown that the hydrogen coverage on supported Rh catalysts is much smaller than the CO coverage. However, as has been demonstrated in the present study on Rh/TiO_2 (W^{6+}) catalysts, the CO coverage can be reduced to a significant extent by weakening the Rh–CO bond via modification of the electronic structure of the Rh crystallites. As has been shown in earlier TPD and FTIR studies (16, 28) carrier doping favors the competitive adsorption of H_2 relative to CO, which results in a relatively high hydrogen coverage, θ_H. According to Eq. [2], higher θ_H values result in an increased rate of CO_2 methanation.

Based on the discussion above, it can be derived that the influence of carrier doping on the activity of CO_2 hydrogenation is related to the weakening of the Rh–CO bond and reduction of CO coverage on the working catalyst surface. As a consequence, hydrogen coverage is increased. This favors the hydrogenation reaction in a twofold way: it increases the concentration of surface hydrogen which participates in the rate-determining step, and it enhances the formation of Rh carbonyl hydride species through which the reaction proceeds via a route with lower activation energy. Therefore, the reduced coverage of the active C_α species on the doped catalysts can also be attributed to

the enhanced hydrogen coverage which favorably consumes the C$_\alpha$ species. The enhanced coverage of the inactive C$_\beta$ species on the doped catalyst should then be related to the increased rate of C–O dissociation (assisted by hydrogen) which proportionally increases the probability for C$_\beta$ formation, originating from the aging of the C$_\alpha$ species. It should be mentioned that the above hypothesis only offers one reasonable explanation of the present observations. Certainly, other possible explanations, e.g., CO activation involving a local interaction like electrostatic or a C and O coordination, cannot be excluded.

Dissociation of the C–O bond is generally believed to be the rate-determining step for CO$_X$ hydrogenation. Earlier results, mainly from surface studies under UHV conditions (45), and from studies of organometallic analogues (46), clearly demonstrate that a correlation exists between the weakening of the C–O bond and the enhancement of CO$_X$ hydrogenation activity. However, as shown in the present study, caution should be exercized when applying such a correlation in practical catalyst systems where the situation is more complicated. Under real conditions of CO$_X$ hydrogenation, a large CO pool will be created on the surface due to the high affinity of CO for metal surfaces. This "unnecessarily" large CO pool would disfavor H$_2$ chemisorption, resulting in reduction of the rate of CO$_X$ hydrogenation. It is recalled that in a study of CO and CO$_2$ hydrogenation over a Ni catalyst, reported by Fujita *et al.* (47), the rate of CH$_4$ formation was found to increase by ca. 20 times when the adsorbed CO formed during the reaction was removed by thermal desorption. Also, it is well-known (5, 22) that the activity of CO$_2$ hydrogenation is significantly reduced by addition of a small amount of gaseous CO, which tends to adsorb strongly on the surface. Therefore, the global observation of the weakening of the Rh–CO bond (or the strengthening of C–O bond) does not mean that the hydrogenation activity is decreased. As revealed by the present study, enhanced hydrogenation activity can be obtained over the catalyst which apparently shows a weaker M–CO bond.

The reason that CO$_2$ methanation, a process which requires the additional reaction step of dissociation of CO$_2$ to adsorbed CO, exhibits higher activity and selectivity towards methane, and enjoys lower activation energy as compared to CO methanation, has been the subject of controversy in the literature (7–9). The present results show that the coverages of adsorbed CO and hydrocarbon fragments on the working catalyst surface under CO$_2$ hydrogenation are significantly lower than those under CO hydrogenation, under analogous reaction conditions (see Table 1 and Fig. 5). This could be attributed to relatively higher hydrogen coverage on the CO$_2$/H$_2$-exposed surface than on the CO/H$_2$-exposed surface. Decreasing CO coverage on the surface, as in the case

of CO$_2$ hydrogenation, implies increased H coverage and, consequently, enhanced removal of surface hydrocarbon fragments and formation of surface carbonyl hydride species. This is at least a partial explanation of the observation that CO$_2$ methanation exhibits higher activity and methane selectivity, and lower activation energy, as compared to CO methanation, in spite of the similar pathways of the two reactions.

CONCLUSIONS

The following conclusions can be drawn from the present investigation of CO and CO$_2$ hydrogenation over Rh/TiO$_2$ (W^{6+}) catalysts.

1. At least five types of carbon-containing species are present on the Rh catalyst surface during the reaction of CO$_X$ ($x = 1$ and 2) hydrogenation, namely: the linearly adsorbed CO, the bridged adsorbed CO, the active carbon (C$_\alpha$), the less active carbon (C$_\beta$) on Rh crystallites, and carbon-containing species (formate and/or carbonate and/or hydrocarbonate) on the TiO$_2$ support.

2. It is confirmed that the Rh–CO bond strength is significantly reduced by doping TiO$_2$ with small amounts of W^{6+} cations. A reduction in CO coverage by 25–40% and a blue shift of the linear CO band by 10–14 cm^{-1} were observed during CO and CO$_2$ hydrogenation over the doped catalysts.

3. In addition to CO coverage, the concentrations of the C$_\alpha$, C$_\beta$, and carbonate and/or hydrocarbonate species are also influenced by carrier doping. The concentration of the C$_\alpha$ (including CH$_X$) species on the Rh crystallites was found to decrease and that of C$_\beta$ was found to increase with increasing dopant content. The concentration of the carbonate and/or hydrocarbonate species, presumably on the carrier, was found to exhibit a maximum at a dopant level of 0.11–0.22 at.%.

4. The enhanced activity and reduced activation energy for CO and CO$_2$ hydrogenation upon carrier doping seems to be related to the observation of the weakening of the Rh–CO bond by carrier doping, presumably due to modification of the electronic structure of the Rh crystallites by carrier doping. Weakening of the Rh–CO bond favors increased hydrogen coverage on the working surface, which has two consequences, namely, increased concentration of surface hydrogen which participates in the rate-determining step and enhanced formation of Rh carbonyl hydride species through which the reaction proceeds via a route of lower activation energy (H-assisted CO dissociation).

5. The CO coverage during CO$_2$ hydrogenation is found to be much smaller than that during CO hydrogenation under analogous conditions. It is proposed that the low CO coverage of the CO$_2$/H$_2$-exposed surface favors enhancement of hydrogen coverage, which leads to increased

activity and selectivity towards methane, and reduced apparent activation energy, as compared to those of the CO/H$_2$-exposed surface.

REFERENCES

1. Vannice, M. A., and Twu, C. C., *J. Catal.* **82**, 213 (1983).
2. Erdöhelyi, A., and Solymosi, F., *J. Catal.* **84**, 466 (1983).
3. Yates, J. T., Thiel, P. A., and Weinberg, W. H., *Surf. Sci.* **84**, 427 (1979).
4. Bertucco, A., and Bennett, C. O., *Appl. Catal.* **35**, 329 (1987).
5. Henderson, M. A., and Worley, S. D., *J. Phys. Chem.* **89**, 1417 (1985).
6. Iisuka, T., Tanaka, Y., and Tanabe, K., *J. Catal.* **76**, 1 (1982).
7. Solymosi, F., Erdöhelyi, A., and Bansagi, T., *J. Catal.* **68**, 371 (1981).
8. Amariglio, A., Lakhdar, M., and Amariglio, H., *J. Catal.* **81**, 247 (1983).
9. Lee, G. V. D., and Ponec, V., *Catal. Rev.* **29**, 183 (1987).
10. Guczi, L., *in* "New Trends in CO Activation" (L. Guczi, Ed.), Studies in Surface Science and Catalysis, Vol. 64, p. 350. Elsevier, Amsterdam, 1991.
11. Sexton, B. A., and Somorjai, G. A., *J. Catal.* **46**, 167 (1977).
12. Solymosi, F., Erdöhelyi, A., and Kocsis, M., *J. Catal.* **65**, 428 (1980).
13. Solymosi, F., Erdöhelyi, A., and Bansagi, T., *J. Chem. Soc. Faraday Trans. 1* **77**, 2645 (1981).
14. Tanaka, Y., Iizuka, T., and Tanabe, K., *J. Chem. Soc. Faraday Trans. 1* **78**, 2215 (1982).
15. Solymosi, F., Tombacz, I., and Konszta, J., *J. Catal.* **95**, 578 (1985).
16. Ioannides, T., and Verykios, X., *J. Catal.* **145**, 479 (1994).
17. Ioannides, T., Verykios, X. E., Tsapatsis, M., and Economous, C., *J. Catal.* **145**, 491 (1994).
18. Zhang, Z. L., Kladi, A., and Verykios, X. E., *J. Catal.* **148**, 737 (1994).
19. Worley, S. D., Mattson, G. A., and Candill, R., *J. Phys. Chem.* **87**, 1671 (1983).
20. Benitez, J. J., Alvero, R., Capitan, M. J., Carrizosa, I., and Odriozola, J. A., *Appl. Catal.* **71**, 219 (1991).
21. Burkett, H. D., Worley, S. D., and Dai, C. H., *Chem. Phys. Lett.* **173**, 430 (1990).
22. Prairie, M. R., Renken, A., Highfield, J. G., Ravindranathan, Thumpi, K., and Grätzel, M., *J. Catal.* **129**, 130 (1991).
23. Bianchi, D., Tau, L. M., Borcar, S., and Bennett, C. O., *J. Catal.* **84**, 358 (1983).
24. Efstathiou, A. M., and Bennett, C. O., *J. Catal.* **120**, 118 and 137 (1989).
25. Bennett, C. O., *in* "Catalysis Under Transient Conditions" (A. T. Bell and L. L. Hegedüs, Eds.), Am. Chem. Soc. Symps. Ser., Vol. 178, p. 1. Am. Chem. Soc., Washington, DC, 1982.
26. Efstathiou, A. M., Chafik, T., Bianchi, D., and Bennett, C. O., *J. Catal.* **147**, 24 (1994); **148**, 224 (1994).
27. Akubuiro, E. C., and Verykios, X. E., *J. Catal.* **103**, 320 (1987); **113**, 106 (1988).
28. Zhang, Z. L., Kladi, A., and Verykios, X. E., *J. Phys. Chem.* **98**, 6804 (1994).
29. Zhang, Z. L., Kladi, A., and Verykios, X. E., *J. Mol. Catal.* **89**, 229 (1994).
30. Efstathiou, A. M., and Bennett, C. O., *Chem. Eng. Commun.* **83**, 129 (1989).
31. Rethwisch, D. G., and Dumesic, J. A., *Langmuir* **2**, 73 (1986).
32. Rice, C. A., Worley, S. D., Curtis, C. W., Guin, J. A., and Tarrer, A. R., *J. Chem. Phys.* **74**, 6487 (1981).
33. Solymosi, F., and Pasztor, M., *J. Catal.* **104**, 312 (1987).
34. Idriss, H., Hindermann, J. P., Kieffer, R., Kiennemann, A., Vallet, A., Chauvin, C., Lavelley, J. C., and Chaumette, P., *J. Mol. Catal.* **42**, 205 (1987).
35. Chauvin, C., Saussey, J., Lavalley, J. C., Idriss, H., Hindermann, J. P., Chaumette, P., and Courty, P., *J. Catal.* **121**, 56 (1990).
36. Angevaare, P. A. J. M., Hendrickx, H. A. C. M., and Ponec, V., *J. Catal.* **110**, 11 (1988).
37. Primet, M., Basset, J. M., Mathieu, M. V., and Prettre, M., *J. Catal.* **29**, 213 (1973).
38. Solymosi, F., Bansagi, T., and Erdöhelyi, A., *J. Catal.* **72**, 166 (1981).
39. Ioannides, T., and Verykios, X. E., *J. Catal.* **140**, 353 (1993).
40. Akubuiro, E. C., and Verykios, X. E., *J. Phys. Chem. Solids* **50**, 17 (1989).
41. Akubuiro, E. C., Ioannides, T., and Verykios, X. E., *J. Catal.* **116**, 590 (1989).
42. Raupp, G. B., and Dumesic, J. A., *J. Catal.* **97**, 85 (1986).
43. Tyagi, M. S., *in* "Metal-Semiconductor Schottky Barrier Junctions and Their Applications" (B. L. Sharma, Ed.), p. 1. Plenum, New York, 1984.
44. Takeuchi, A., Katzer, J. R., and Schuit, G. C. A., *J. Catal.* **82**, 477 (1983).
45. Boff, A. B., Lin, C., Bell, A. T., and Somorjai, G. A., *Catal. Lett.* **27**, 243 (1994).
46. Horwitz, C. P., and Shriver, D. F., *Adv. Organomet. Chem.* **23**, 219 (1984).
47. Fujita, S., Terunuma, H., Nakamura, M., and Takezawa, N., *Ind. Eng. Chem. Rev.* **30**, 1146 (1991).